Astron. Astrophys. 315, L257–L260 (1996)

ASTRONOMY AND ASTROPHYSICS

The ISO LWS grating spectrum of NGC 7027

X.-W. Liu[1], M.J. Barlow[1], Nguyen-Q-Rieu[2], Truong-Bach[2], P. Cox[3], D. Péquignot[4], P.E. Clegg[5], B.M. Swinyard[6], M.J. Griffin[5], J.P. Baluteau[7], T. Lim[8], C.J. Skinner[9], H.A. Smith[10], P.A.R. Ade[5], I. Furniss[1], W.A. Towlson[1], S.J. Unger[6], K.J. King[6], G.R. Davis[11], M. Cohen[12], R.J. Emery[6], J. Fischer[13], W.M. Glencross[1], E. Caux[14], M.A. Greenhouse[10], C. Gry[7,8], M. Joubert[15], D. Lorenzetti[16], B. Nisini[17], A. Omont[18], R. Orfei[17], P. Saraceno[17], G. Serra[14], H.J. Walker[6], C. Armand[8], M. Burgdorf[8], A. Di Giorgio[8], S. Molinari[8], M. Price[8], D. Texier[8], S. Sidher[8], and N. Trams[8]

[1] Department of Physics and Astronomy, University College London, Gower Street, London WC1E 6BT, UK
[2] Observatoire de Paris, 61 avenue de l'Observatoire, F-75014 Paris, France
[3] Institut d'Astrophysique Spatiale, Bât. 120, Université Paris XI, F-91405 Orsay, France
[4] Observatoire de Paris-Meudon, F-92190 Meudon, France
[5] Department of Physics, Queen Mary and Westfield College, Mile End Road, London E1 4NS, UK
[6] Space Science Department, Rutherford Appleton Laboratory, Chilton, Oxon OX11 0QX, UK
[7] Laboratoire d'Astronomie Spatiale, CNRS, BP 8, F-13376 Marseille Cedex 12, France
[8] The LWS Instrument-Dedicated Team, ISO Science Operations Center, P.O. Box 50727, E-28080 Madrid, Spain
[9] Space Telescope Science Institute, 3700 San Martin Drive, Baltimore, MD 21218, USA
[10] National Air and Space Museum, Smithsonian Institute, Laboratory for Astrophysics, Washington, DC 20560, USA
[11] Institute of Space and Atmosphere Studies, University of Saskatchewan, 116 Science Place, Saskatoon, Saskatchewan, Canada S7N 5E2
[12] Radio Astronomy Laboratory, 601 Campbell Hall, University of California, Berkeley, CA 94720, USA
[13] Naval Research Laboratory, Remote Sensing Division, 4555 Overlook Ave, SW, Washington, DC 20375, USA
[14] Centre d'Etude Spatiale des Rayonnements, CESR/CNRS-UPS, BP 4346, F-31029 Toulouse Cedex, France
[15] CNES, 2 place Maurice Quentin, F-75001 Paris, France
[16] Osservatorio Astronomico di Roma, I-00040 Monte Porzio, Italy
[17] CNR-Istituto di Fisica dello Spazio Interplanetario, Casella Postale 27 I-00044 Frascati, Italy
[18] Institut d'Astrophysique, 98bis boulevard Arago, F-75014 Paris, France

Received 16 July 1996 / Accepted 19 August 1996

Abstract. We present a high signal-to-noise ISO Long Wavelength Spectrometer (LWS) grating spectrum of the planetary nebula NGC 7027 from 43–194μm. In total 40 emission lines have been detected, with 30 identified. From the ionized region, we observe fine-structure lines from [N II], [N III] and [O III]. The [O I] and [C II] fine-structure lines from the photodissociation region are the strongest features observed in this spectral region. Amongst the molecular lines, 11 pure rotation CO lines from J=14–13 up to J=24–23 have been detected. The most striking result, however, is the detection in this carbon-rich nebula of the o-H_2O 179.53μm and the OH 119.3μm fundamental lines. Astrophysical implications are briefly discussed.

Key words: planetary nebulae: general – planetary nebulae: individual: NGC 7027 – ISM: atoms – ISM: molecules

1. Introduction

NGC 7027 is the most widely studied planetary nebula (PN) due to its very rich (and bright) spectrum, in both atomic and molecular lines. It is a young, dense PN with a hot central star ($T_{\rm eff} \gtrsim 140\,000$ K). Optical and UV spectroscopy shows that it is C-rich with a C:O ratio of 2.2 ± 0.2 (Middlemass 1990, M90 hereafter; Gruenwald & Péquignot 1989, GP89 hereafter). The ionized regions, partly obscured by heavy circum-nebular dust extinction (M90), are surrounded by a massive molecular envelope. NGC 7027 was the first PN to be detected in both CO and H_2 emission (Mufson et al. 1975; Treffers et al. 1976), and subsequently in various other molecules, including HCN, CN, C_3H_2, HCO^+, N_2H^+, and CO^+, pointing to a rich on-going ion-molecule dominated chemistry. It was the first object found to exhibit the now well-known UIR bands (Gillett et al. 1973), which have been attributed to aromatic molecular species. KAO observations revealed strong [O I] 63μm, 146μm and [C II] 158μm emission lines from the photodissociation region (PDR), the interface between the ionized nebula and its molecular envelope (Ellis & Werner 1984). Here we present a high signal-to-noise grating spectrum of NGC 7027 between 43 and 194μm, obtained with the LWS (Clegg et al. 1996) on board the Infrared Space Observatory (ISO; Kessler et al. 1996).

Send offprint requests to: X.-W. Liu (xwl@star.ucl.ac.uk)

[1] Based on observations with ISO, an ESA project with instruments funded by ESA Member States (especially the PI countries: France Germany, the Netherlands and the United Kingdom) and with the participation of ISAS and NASA.

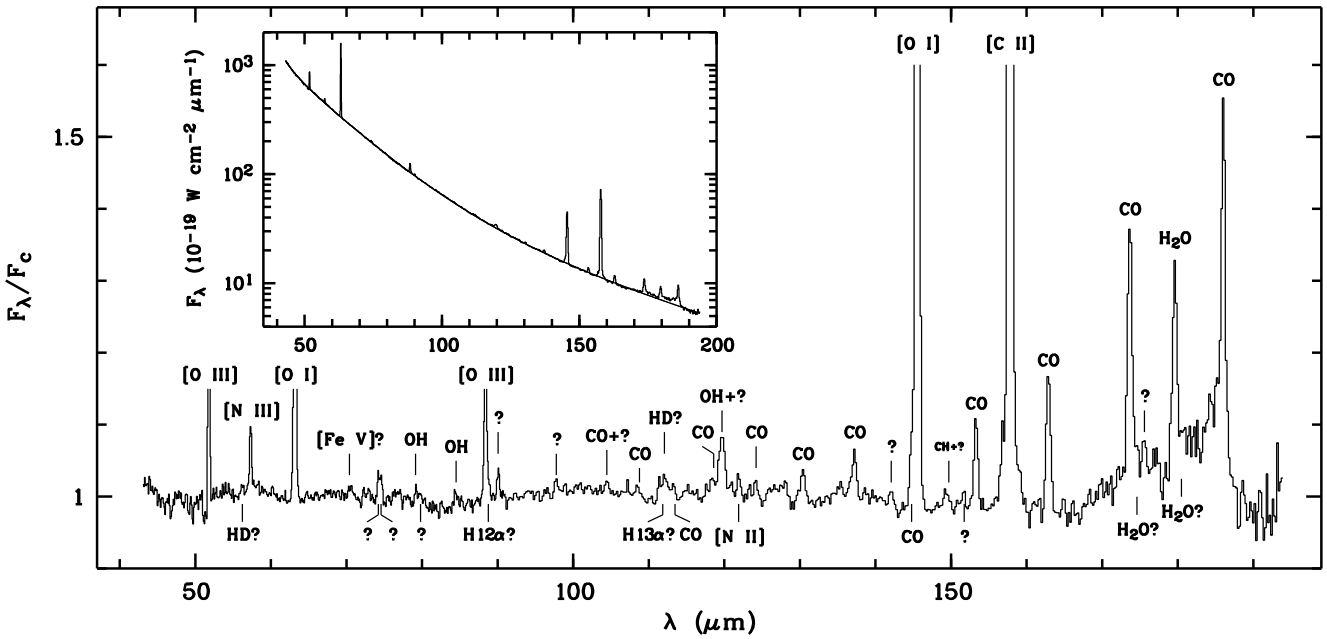

Fig. 1. The ISO LWS spectra of NGC 7027 between 43–194μm, after division by a fifth order polynomial fit in the log F_λ − log λ plane to the continuum, with detected features labelled. The complete spectrum before normalization by the continuum fit is shown in the insert.

2. Observations

The data described here were obtained during the Performance Verification Phase of ISO, in Revolution 39 (December 27, 1995), using a non-standard LWS observation mode (COIF). Three observations were made, each consisting of 5 full grating scans with two 0.5 sec integration ramps at each grating position. The spectra were sampled at 1/15 of a spectral resolution element, the latter being 0.3μm in second order (SW1–SW5; $\lambda \lesssim 93\mu$m) and 0.6μm in first order (LW1–LW5; $\lambda \gtrsim 80\mu$m). The total on-target time was 14520 sec. The spectra were flux calibrated relative to Uranus (Swinyard et al. 1996). The sub-spectra from the ten LWS detectors have significant overlaps in wavelength and small scaling factors have been applied such that they joined smoothly to form a complete spectrum from 43–194μm. The mean scaling factor was 0.05 dex, except for SW1, where a scaling factor of -0.21 dex was used.

3. Results

The complete spectrum after merging the sub-spectra from the ten detectors is presented in the insert in Fig. 1, together with fit to the continuum level. Over the observed wavelength range, the dust continuum increases sharply towards shorter wavelengths by more than two orders of magnitude in F_λ. No definite broad emission/absorption bands characteristic of dust features are detected, in strong contrast to the near- and mid-infrared wavelength region. There is however an apparent rise in the continuum longwards of 165μm until 185μm, where it returns to the underlying level again (Fig. 1), a phenomenon not seen in any other LWS spectra so far. It could be due to a broad feature, or to the blending of multiple emission lines. The emission lines detected and their fluxes are given in Table 1. In total 40 lines are listed, with 30 identified. To illustrate better the weak features, the same spectrum normalized by the fitted continuum is plotted in Fig. 1, with detected lines labelled.

1) Lines from the ionized region: In the high electron density environment of NGC 7027, ionic fine-structure lines are strongly suppressed by collisional de-excitation. The [O III] 52μm and 88μm lines have a flux ratio of 9.3, which is within 10 per cent of its high density limit. In the model for NGC 7027 presented by GP89 (central star: $T_{\rm eff}$ = 1.9×10^5 K and L = 9500 $L_\odot$ at a distance of 1 kpc), the ionized region extends from 2 to 4 arcsec and the mean electron density $n_{\rm e}$ and temperature $T_{\rm e}$, weighted by O^{2+} ions, are 7.1×10^4 cm^{-3} and 1.3×10^4 K, respectively. The predicted strengths of the IR [N II] and [O III] lines, relative to the optical forbidden lines and the UV intercombination lines, are too great by a factor $\sim$ 1.45 (adopting $O^{2+}/H^+ = 2.3\times10^{-4}$; GP89). However, the [N II] 122μm line is faint and good agreement is found between the observations and the model in the case of the N III] 0.1749μm/[N III] 57μm ratio. The discrepancy concerning the [O III] lines may suggest that $n_{\rm e}$ is incorrect in the GP89 model. Nonetheless $n_{\rm e}$ is also 7×10^4 cm^{-3} in the model of Keyes et al. (1990), whereas in the model of M90 the density of 5×10^4 cm^{-3} would predict even higher [O III] IR line fluxes. Alternatively, the discrepancy may indicate the presence of strongly obscured material that shows up only in the IR (see the differential extinction model proposed by M90).

2) Atomic lines from the PDR: The [O I] 63μm, 146μm and the [C II] 158μm fine-structure lines, the dominant cooling lines of the PDR, have been detected previously by the KAO (Ellis & Werner 1984), with reported fluxes of (32 ± 10), (1.2 ± 0.4) and (3.4 ± 1.0) × 10^{-18} W cm^{-2}, respectively, in agreement with the ISO LWS measurements within the quoted errors. For a given C:O abundance ratio, Watson (1983) has shown that the λ63μm/λ146μm and λ63μm/λ158μm ratios can be used to

Table 1. LWS far-infrared emission line fluxes from NGC 7027

$\lambda_{vac}(\mu m)$	Identification	Det	$\lambda_{obs}(\mu m)$	Flux[a]
51.82	[O III]	SW2	51.78	886.
56.23	HD (0,0) R(1)[b]	SW2	56.24	16.3[c]
"	"	SW3	56.22	22.8[c]
57.33	[N III]	SW2	57.30	175.
"	"	SW3	57.31	162.
63.18	[O I]	SW2	63.17	4360
"	"	SW3	63.17	3980
?	?	SW4	74.22	24.1
?	?	SW4	74.58	22.1
79.15	OH $^2\Pi_{1/2}$J=$\frac{1}{2}$–$^2\Pi_{3/2}$J=$\frac{3}{2}$	SW5	79.20	14.0[c]
?	?	SW5	79.81	15.1[c]
84.51	OH $^2\Pi_{3/2}$ J=7/2–5/2	SW5	84.48	17.3[c]
?	?	SW5	86.14	6.54[c]
88.36	[O III]	SW5	88.40	97.9
"	"	LW1	88.35	92.3
88.76	H 12α[b]	SW5	88.80	9.26[c]
?	?	SW5	90.08	21.6
"	"	LW1	90.06	12.6
?	?	LW1	97.76	9.26[c]
104.44	CO (0,0) J=25–24+?	LW2	104.44	9.56[c]
108.76	CO (0,0) J=24–23	LW2	108.77	4.80[c]
111.86	H 13α[b]	LW2	111.86	3.52[c]
112.07	HD (0,0) R(0)[b]	LW2	112.07	8.75[c]
113.46	CO (0,0) J=23–22	LW2	113.46	3.03[c]
118.58	CO (0,0) J=22–21	LW2	118.58	5.13[c]
119.34	OH $^2\Pi_{3/2}$ J=5/2–3/2 +?	LW1	119.68	27.1
"	"	LW2	119.71	30.4
121.90	[N II]	LW2	121.89	5.34[c]
"	"	LW3	121.88	7.41[c]
124.19	CO (0,0) J=21–20	LW2	124.19	3.25[c]
"	"	LW3	124.17	4.95[c]
130.37	CO (0,0) J=20–19	LW3	130.35	8.44
137.20	CO (0,0) J=19–18	LW3	137.18	12.1
?	?	LW3	142.12	2.93[c]
"	"	LW4	142.04	3.14[c]
144.78	CO (0,0) J=18–17	LW3	144.80	9.04[c]
"	"	LW4	144.79	6.45[c]
145.52	[O I]	LW3	145.54	187.
"	"	LW3	145.53	188.
149.24	CH $^2\Pi_{1/2}$ (0,0) J=$\frac{3}{2}$–$\frac{1}{2}$[b]	LW3	149.23	2.08[c]
?	?	LW3	149.94	2.11[c]
?	?	LW3	151.73	3.60[c]
153.27	CO (0,0) J=17–16	LW3	153.27	10.0
"	"	LW4	153.30	13.0
157.74	[C II]	LW3	157.76	355.
"	"	LW4	157.80	382.
"	"	LW5	157.75	318.
162.81	CO (0,0) J=16–15	LW4	162.84	17.8
"	"	LW5	162.82	14.5
173.63	CO (0,0) J=15–14	LW5	173.66	21.2
174.61	o-H_2O (0,0) 3_{03}–2_{12}[b]	LW5	174.64	2.21[c]
?	?	LW5	175.59	2.76[c]
179.53	o-H_2O (0,0) 2_{12}–1_{01}	LW5	179.56	13.8
180.49	o-H_2O (0,0) 2_{21}–2_{12}[b]	LW5	180.52	2.18[c]
186.00	CO (0,0) J=14–13	LW5	186.02	22.5

[a] in 10^{-20} W cm^{-2}; [b] identification questionable; [c] weak & noisy.

derive the temperature and density in the PDR. For NGC 7027, if we assume C:O = 2, the line ratios measured by ISO (and by the KAO) fall in the high temperature area of the diagnostic diagram where they are no longer sensitive to temperature variations. In fact, for C:O$\sim$ 2 the observed ratios (with an estimated uncertainty of 15 per cent) would suggest $T > 2000$ K, much too high compared to the typical value of 1000 K found for the PDR. One possibility is that the two [O I] lines, in particular the λ63 μm line, are optically thick. For T = 1000 K and assuming thermal broadening only, an H I column density of $\sim 10^{21}$ cm^{-2} ($A_V \sim 0.5$ mag) will yield unit optical depth for the $\lambda 63\mu$m and $\lambda 146\mu$m lines. Assuming that the [C II] 158μm line (which requires higher H I column densities to become optically thick than do the [O I] lines) is optically thin and that C^+ is the dominant form of carbon, then for C/H = 1×10^{-3} (GP89, M90) and a distance to NGC 7027 of 700 pc (Hajian et al. 1993), we find a total mass (H + He nuclei) of 0.125 $M_\odot$ for the PDR, ten times smaller than the mass of the cold molecular envelope seen in mm-wave CO lines (Jaminet et al. 1991; J91 hereafter).

3) Molecular lines: Eleven CO pure rotational lines have been detected, from J=14–13 up to J=24–23 (A weak feature is detected at 104.44 μm, coincident in wavelength with the CO J=25–24 line. However, it appears to be too strong as compared to other CO lines detected and thus could be a blend). Their fluxes are plotted in Fig. 2 against Ju. Also shown are fluxes for the J=3–2, 2–1 and 1–0 lines (compiled from various mapping data) and the J=17–16 line as measured with the KAO by Justtanont et al. (1995). Assuming an emitting slab of uniform temperature and density, the relative fluxes of the high-J CO lines measured by ISO are best fitted using T = 1000 K and $n(H_2) = 10^5$ cm^{-3}. A (slightly inferior) fit can also be achieved with T = 700 K and $n(H_2) = 10^6$ cm^{-3}. For comparison, we also show the emissivities of CO lines from a slab of the same density but with a temperature of T = 30 K, characteristic of the low-J CO mm-wave lines (J91), normalized to the J=1–0 line, which is only moderately optically thick (J91). Fig. 2 shows that the high-J CO lines originate from the warm PDR, where the molecules are rapidly photodissociated and have a typical temperature of around 1000 K. The total number of CO molecules in the PDR is estimated to be 1.6×10^{51}, only 2 per cent of the total number of C^+ ions in the same region as derived from the [C II] 157μm line (see above). As expected, most of the CO molecules in the warm PDR have been dissociated.

Theoretical PDR calculations by Burton et al. (1990) show that the relative fluxes of the FIR and mm-wave CO lines provide a sensitive diagnostic for the FUV radiation field and gas density. In their PDR model for NGC 7027, which consists of two components, one of n(H) = 10^5 cm^{-3} and G_0 = 10^5 and another of n(H) = 10^6 cm^{-3} and G_0 = 10^5, with the former contributing 2/3 of the total emission, the predicted [O I]λ63μm/[C II]λ157μm line ratio and the CO J=16–15 to J=1–0 line ratio are respectively a factor of 3 and 6 lower than observed. Comparison of Fig. 2 with their Fig. 5 indicates a FUV radiation field of $10^4 \lesssim G_0 \lesssim 10^5$ and a density of $10^6 \lesssim n(H) \lesssim 10^7$ cm^{-3}. Such a density is much higher than the value of 10^5 cm^{-3}, which best fits the relative emissivity distribution of the high-J

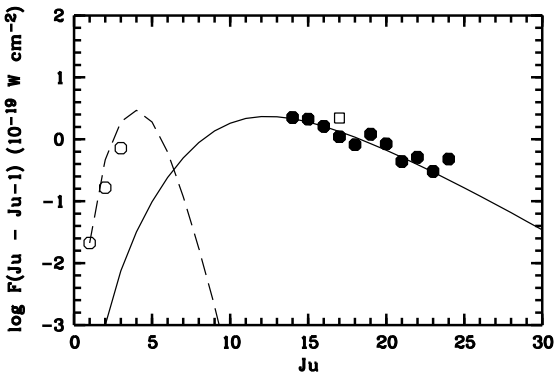

Fig. 2. CO pure rotational line fluxes measured by ISO's LWS (filled circles), the KAO (open box) and ground-based mm-wave observations (open circles), plotted against the rotational quantum number of the upper level, Ju. The solid and dashed lines show the flux distributions of the CO lines as a function of Ju in an equilibrium slab of uniform temperature of 1000 K (normalized to the J=16-15 line) and of 30 K (normalized to the J=1-0 line). In both cases an H_2 density of 10^5 cm^{-3} and a He:H_2 abundance ratio of 0.2 by number have been assumed.

CO lines (Fig. 2), but seems to be consistent with the constraints imposed by the OH and H_2O lines, discussed below.

The most surprising result from these ISO LWS observations is the discovery in this C-rich nebula of the o-H_2O 179.53μm and OH 119.3μm fundamental lines, which have excitation energies of $T_{\rm ex}$ = 80 and 120 K, respectively (it is noteworthy that this was the first spectrum in which a FIR water vapour emission line was detected). The OH 119.3μm line is blended with an unidentified feature. From Gaussian line profile fitting (note that due to Λ-doubling, the OH 119μm line itself consists of two components separated by 0.2μm), we estimate fluxes of 1.34 and 1.53×10^{-19} W cm^{-2} for the OH line and the unidentified line (at $119.89\pm0.05\mu$m), respectively. In addition to the fundamental line, two other OH lines have been tentatively detected, the 79.15μm ($T_{\rm ex}$ = 182 K) and 84.51μm ($T_{\rm ex}$ = 290 K) lines. For o-H_2O, apart from the fundamental transition, the next two observable lines of lowest excitation energy are at 174.61μm ($T_{\rm ex}$ = 162 K) and 180.49μm ($T_{\rm ex}$ = 160 K), both blended with a much stronger line. Evidence for the presence of these two H_2O lines is however provided by the asymmetric profiles of the features, though their fluxes, derived from profile fitting, are quite uncertain (Table 1).

The chemistry leading to the formation of significant amounts of OH and H_2O molecules in a C-rich environment is uncertain. We are inclined to discount the possibility that the H_2O and OH emission arises in a hypothetical cold ($T\sim30$ K) oxygen-rich outer zone for the following reasons: (a) a deep search by us with the IRAM 30-m telescope has failed to detect SiO 130.27 GHz J = 3–2 line emission down to a sensitivity level of 10 mK; (b) OH emission lines with excitation energies of 182 K and 290 K above the ground state are probably detected (see above); (c) radicals such as HCO^+, N_2H^+ and CO^+ have previously been identified as originating in the warm PDR (e.g. Cox et al. 1993), suggesting that OH and H_2O also originate in this chemically active region. One possibility is that at the elevated temperatures in the PDR, the endothermic reactions O + H_2 $\rightarrow$ OH + H (with O released by CO photodissociation) and OH + H_2 $\rightarrow$ H_2O + H could yield appreciable abundances of OH and H_2O despite the strong photodissociating radiation field. In this scenario, the OH and H_2O lines would come from the warm PDR with a temperature of $\sim$ 1000 K.

For pure collisional excitation and a density of $n(H_2)\sim10^5$ cm^{-3} (§3.2), Large Velocity Gradient model calculations predict that the size of the H_2O emitting region would greatly exceed that of the NGC 7027 PDR (20×11 arcsec^2 in the near-IR lines of H_2; Cox et al. 1996). Moreover several line optical depths would then be large, resulting in lines from levels with $T_{\rm ex}\sim200$ K, such as 138.53, 108.08, and 113.54μm, exceeding 20-40% of the strength of the 179.5μm line, in contradiction with observation. An alternative possibility is emission from a $n(H_2)\sim10^6$cm^{-3} medium at $T\sim1000$ K. The emitting region size can then be reduced to an acceptable value and only the 179.5μm line is thick ($\tau\sim5$) whilst other lines are still thin, with predicted intensities not exceeding 10% of that in the 179μm line. The abundance of H_2O cannot be accurately derived from the optically thick 179.53μm line – a good detection of an optically thin H_2O line is instead required. A temperature of 1000 K is consistent with the production of the observed OH and H_2O molecules by endothermic reactions with H_2 of the oxygen atoms liberated by the photodissociation of CO. We note that the relatively high density of $n(H_2)\sim10^6$ cm^{-3} is plausible, in that it corresponds to approximate pressure equilibrium with the inner ionized region.

Finally, there is marginal evidence for emission from the CH 149μm line, the HD 56 and 112μm fundamental lines, and from the H I recombination lines H 12α and H 13α (Table 1). Fabry-Perot observations are required to confirm these detections.

References

Burton M.G., Hollenbach D. J., Tielens A.G.G.M., 1990, ApJ 365, 620
Clegg P. E., et al., 1996, this volume
Cox P., Bachiller R., Huggins P. J., Omont A., Guilloteau S., 1993, Planetary Nebula, eds R. Weinberger & A. Acker, Kluwer, p.227
Cox P., et al., 1996, A&A in press
Ellis H. B., Werner M. W., 1984, BAAS 16, 463
Gillett F. C., Forrest W. J., Merrill K. M., 1973, ApJ 183, 87
Gruenwald R.B, Péquignot D., 1989, IAU Symposium 131, Planetary Nebulae, ed. S. Torres-Peimbert, Kluwer, Dordrecht, p. 224 (GP89)
Hajian A. R., Terzian Y., Bignell C., 1993, AJ 106, 1965
Jaminet P. A., Danchi W. C., Sutton E. C., Russell A. P. G., Sandell G., Bieging J. H., Willner D., 1991, ApJ 380, 461 (J91)
Kessler M. F., et al., 1996, this volume
Justtanont K., Tielens A. G. G. M., Skinner C. J., Haas M. R., 1995, in Airborne Astronomy Symp. on the Galactic Ecosystem, ASP Conf. Ser., Vol. 73, eds M. R. Haas, J. A. Davidson, E. F. Erickson, p.429
Keyes C.D., Aller L.H., Feibelman W.A., 1990, PASP 102, 59
Middlemass D., 1990, MNRAS 244, 294 (M90)
Mufson S. L., Lyon J., Marionni P. A., 1975, ApJ 201, L85
Swinyard B. M., et al., 1996, this volume
Treffers R.R., Fink U., Larson H.P., Gautier T.N., 1976, ApJ 209, 793
Watson D. M., 1983, in Galactic & Extragalactic Infrared Spectroscopy, eds M. F. Kessler & J. P. Phillips, Reidel, p.193